Isotopic fractionation in the proto-lunar disk: constraints on equilibration

Kaveh Pahlevan[1,*], Charles Gammie[2]

1. School of Earth and Space Exploration, Arizona State University, Tempe, AZ, 85281
2. Department of Astronomy, University of Illinois, 1002 West Green Street, Urbana, IL, 61801

Email: kaveh.pahlevan@asu.edu

Tel: +1 480 401 8584

5 Figures

To be submitted to EPSL

Abstract

Despite its importance to questions of lunar origin, the evolution of the proto-lunar disk has eluded a precise description. A number of recent developments have nevertheless made it possible to constrain this evolution. Here, we use a physical-chemical model of the proto-lunar disk with a silicate vapor atmosphere and a separately convective magma layer to explore the consequences of turbulent mixing across the radial extent of the disk. Four features of such a stratified turbulent disk act in concert to radially separate the isotopes (e.g. of silicon) by mass: (i) the melt-vapor interface exhibits a temperature gradient across the radial extent of the disk, (ii) silicon exists as SiO_4^{-4} in the melt and primarily as SiO in the co-existing vapor, with the difference in bonding environment resulting in relatively large equilibrium isotopic fractionation (~0.5 per mil difference in $^{30}Si/^{28}Si$) between the two phases, (iii) thermodynamic equilibrium between a magma layer and a co-existing atmosphere – if attained – will therefore tend to concentrate the heavy isotopes into the magma layer, generating an atmosphere that is isotopically light, with the magnitude of isotopic difference dependent on temperature. Radial temperature gradients will, in this way, be translated – through equilibrium partitioning – to gradients in the isotopic composition of the magma layer and the complementary atmosphere, and (iv) turbulent radial mixing in the atmosphere will therefore result in radial isotopic transport, which, in the case of silicon, would tend to concentrate the heavy (light) isotopes in the outer (inner) regions of the disk. That the inner disk material accretes back onto the Earth while the outer disk participates in lunar accretion permits such a redistribution process to be expressed in the isotopic composition of the silicate Earth and Moon. The current precision with which the silicon isotopic composition of these reservoirs is known constrains the degree to which the proto-lunar disk could have existed in such a stratified diffusive regime. These results suggest that – if post-impact Earth-disk equilibration is the cause of the

remarkable isotopic homogeneity observed in the Earth-Moon system – the liquid in the proto-lunar disk must have been entrained into the overlying convective atmosphere and have participated in the turbulent mixing process. Consequences for the post-impact evolution are discussed.

Keywords: Moon, origin, proto-lunar disk, equilibration, isotopes

1. Introduction

The Moon is generally thought to have formed from a melt-vapor disk generated via the off-center impact of a planet-sized body with the proto-Earth towards the end of Earth accretion (Cameron and Ward, 1976; Hartmann and Davis, 1975). Such an origin via giant impact can explain the angular momentum present in the Earth-Moon (EM) system (Cameron and Ward, 1976), the lunar mass and Fe deficit (Canup and Asphaug, 2001), and the small but non-zero inclination of the lunar orbit (Ćuk et al., 2016; Pahlevan and Morbidelli, 2015; Touma and Wisdom, 1998; Ward and Canup, 2000). In its simplest formulation, however, the giant impact model cannot readily explain the precise isotopic similarities observed between the silicate Earth and Moon (Kruijer et al., 2015; Pahlevan, 2014; Touboul et al., 2015; Young et al., 2016) as most of the material that is injected into orbit is sourced from the impacting planet rather than the proto-Earth, a robust feature seen in all simulations of impacts that leave the system with its current level of angular momentum (Canup, 2004, 2008; Canup and Asphaug, 2001; Canup et al., 2013). Here, we refer to the low-velocity, oblique, Mars-mass impact onto the proto-Earth as the "standard" impact.

Motivated by the problem of isotopic homogeneity in the EM system, three new single-impact scenarios have been proposed. First, it has been suggested that the Moon-forming impact was a

hit-and-run event (Reufer et al., 2012) such that the impact could be characterized by more angular momentum than is currently present in the EM system, with the excess being carried off by the impacting body. Such an impact is capable of sourcing a somewhat higher percentage of the proto-lunar disk from Earth's mantle (~60%) than the standard scenario (~40%) and while this reduces the severity of the isotopic problem, it is unlikely to eliminate it entirely. Second, it has been suggested that the proto-Earth was rotating near the threshold for fission before the impact – with a < 3 hour rotation period – and that a high-velocity impactor struck it nearly head-on sourcing a satellite-forming disk directly from proto-Earth's mantle. Finally, it has been proposed that the Moon-forming event may have been a nearly symmetric impact between two ~½ Earth-mass bodies (Canup, 2012). In such a scenario, both the emerging planet and the disk injected into circumplanetary orbit are sourced – by symmetry – equally from the two merging bodies. These last two scenarios have the potential to generate planet-satellite systems with close isotopic similarities, at least for the lithophile elements (Halliday, 2012). However, both scenarios generate planet-satellite systems with a large overabundance of angular momentum – by a factor of 2 or greater – relative to the modern EM system. Hence, to be reconciled with the observed dynamical state of the EM system, most of the angular momentum in these systems must be transferred out; the only mechanisms known that have the potential to remove this amount of angular momentum from a planet-satellite system are the evection resonance (Ćuk and Stewart, 2012; Touma and Wisdom, 1998), a related limit cycle (Tian et al., 2017; Wisdom and Tian, 2015), or the Laplace plane instability (Atobe and Ida, 2007; Ćuk et al., 2016). The efficacy of these mechanisms, however, depends on specific values of the tidal dissipation parameters of the post-impact Earth and nascent Moon that are likely variable during this epoch in the crystallizing planet and satellite and currently not well-constrained.

A different kind of solution to the problem of EM isotopic homogeneity – called equilibration – envisions a proto-lunar disk that is initially isotopically distinct and invokes fluid dynamical mixing of the hot, convective, planet-disk system into a single isotopic reservoir during the ~10^3 years after the giant impact but before the cessation of lunar accretion (Pahlevan and Stevenson, 2007). Since the Moon accretes from the outermost disk material (Salmon and Canup, 2012), such a scenario requires that the proto-lunar disk undergo turbulent mixing across its radial extent. For turbulent viscous-diffusive disks, efficient radial mixing is possible when the turbulent diffusivity (D) is much greater than turbulent viscosity (ν), with the precise numerical requirement depending on the precise magnitude of the required mixing (Stevenson, 1990).

Here, we show that turbulent radial mixing in a stratified proto-lunar disk – with a silicate vapor atmosphere and a separately convective magma layer co-existing in equilibrium – makes specific predictions for mass-dependent isotopic offsets in the composition of lunar and terrestrial silicates. We then use the measured isotopic abundances to set constraints on how the proto-lunar disk could – and could not – have evolved. Finally, we discuss implications for equilibration as the origin of the EM isotopic homogeneity.

2. Disk Model

Currently considered scenarios for a single Moon-forming giant impact (Canup, 2004, 2008, 2012; Canup and Asphaug, 2001; Ćuk and Stewart, 2012; Reufer et al., 2012) shock heat and disaggregate the lunar-forming material into a hot, melt-vapor circumterrestrial disk (Nakajima and Stevenson, 2014). At present, no model exists that begins with such an initial state and follows

93 the evolution, ending with statements about the stable isotopic composition of the lunar-forming
94 material. Here, we describe a numerical disk model with the goal of forging a link between disk
95 processes and observable stable isotopic signatures.
96
97 2.1. Vertical structure
98 The melt-vapor disk generated by the giant impact settles into a nearly hydrostatic state – with a
99 vapor cloud expanding to assume a density distribution according to the local scale height – on
100 dynamical timescales of hours to days. Radiative cooling subsequently drives the evolution of the
101 proto-lunar disk. Vigorous turbulent convection in the atmosphere is required to match high
102 radiative losses from a ~2,000 K photosphere (Thompson and Stevenson, 1988), above which the
103 thermal structure is determined by radiative transfer. Calculation of the disk vertical structure is
104 simplified by the fact that a negligible fraction of the atmospheric mass exists above the
105 photosphere (at ~millibar pressures) with the convective atmosphere extending down to pressures
106 of hundreds of bars (Thompson and Stevenson, 1988). The disk atmosphere is almost entirely
107 convective and, in analogy with planetary atmospheres, is expected to be characterized by an
108 adiabatic (or pseudoadiabatic) vertical structure (Holton, 1992).
109
110 A major unresolved question – which has consequences for lunar composition – is whether the
111 liquid in the proto-lunar disk exists as droplets kept in suspension via vigorous convective motions
112 (Thompson and Stevenson, 1988) or whether the liquid settles into a liquid-rich mid-plane layer
113 that dynamically decouples from the overlying atmosphere (Machida and Abe, 2004; Ward, 2012).
114 We refer to these two cases as the unstratified and stratified disks, respectively. An end-member
115 stratified disk scenario (herein called “fully stratified”) is one in which, not only is the mid-plane

more liquid-rich than would be expected based on a single vertical disk isentrope, but the exchange of matter between the convective liquid layer and the atmosphere is mediated by exchange of atoms across a phase boundary, with no advective fluid motions carrying atoms directly between the two layers (e.g. no convective overshoot). In such a fully stratified scenario, elements that readily vaporize (e.g. O) will enter the atmosphere, and be available to undergo radial mixing and isotopic equilibration (Pahlevan and Stevenson, 2007) while the more refractory elements (e.g. Ti) will be concentrated in the mid-plane liquid layer and may undergo less Earth-disk equilibration. EM isotopic heterogeneity for refractory elements has been sought, but not found (Zhang et al., 2012), although hints of such heterogeneity may recently have been observed in calcium isotopes (Schiller et al., 2018).

Here, we assume that the disk is fully stratified: that the vertical structure consists of a convective liquid-rich mid-plane layer, a liquid-vapor interface, and an overlying convective atmosphere. The separately convective liquid-rich and vapor-rich columns are assumed to be in thermodynamic equilibrium at precisely defined interface conditions. Vertical mixing *within* each layer is assumed to be efficient because convective velocities are high and variations in atmospheric composition due to phase separation ("rainout") are expected to be small relative to the composition contrast between the liquid-rich layer and vapor-rich atmosphere (Pahlevan et al., 2011). Implications of relaxing the assumption of efficient vertical mixing are discussed in §4.2.

The pressure at the liquid-vapor interface is determined by hydrostatic balance with both the self-gravity of the disk and the vertical component of central planetary gravity:

$$-\frac{1}{\rho}\frac{\partial P}{\partial z} = 2\pi G\sigma(z) + \frac{GM_E}{r^3}z \qquad (1)$$

where ρ is the density, P is the pressure, z is the height above the mid-plane, G is the gravitational constant, σ(z) is the local disk surface density enclosed at height z, M_E is the mass of the Earth, and r is the radial distance in cylindrical coordinates. This equation can be integrated to yield:

$$P_{\text{int}} = \frac{\pi G \sigma_T^2}{2}\left[1-(1-f_v)^2\right] + \frac{1}{2}\Omega^2 \sigma_T f_v h_{mass} \qquad (2)$$

where P_{int} is the interface pressure, σ_T is the total surface density of the column (liquid layer plus atmosphere), f_v is the mass fraction of the vapor atmosphere in the column ($\equiv\sigma_v/\sigma_T$), Ω is the Keplerian angular velocity [$\equiv(GM_E/r^3)^{1/2}$], and h_{mass} is the mass-weighted scale height of the column which, for even moderate vapor fractions (f_v), can be approximated as the mass-weighted height of the vapor atmosphere:

$$h_{mass} = 2\int_{z_{\text{int}}\approx 0}^{\infty} z\rho_v(z)dz \Big/ \int_{-\infty}^{\infty} \rho_v(z)dz \qquad (3)$$

We assume that the second term in equation (2) corresponding to the vertical component of Earth's gravity dominates, such that $h_{mass} \sim c_s/\Omega$, where c_s is the isothermal sound speed [$\equiv(kT/\mu)^{1/2}$] and μ is the mean molecular weight of the vapor. By subsequently substituting nominal parameter values for the proto-lunar disk ($\sigma_T = 5\text{x}10^6$ g/cm^2, $\Omega = 2\text{x}10^{-4}$ s^{-1}, $c_s = 10^5$ cm/s) into both terms in equation (2), the dominance of the central gravity term in determining the disk vertical structure can be confirmed. This calculation justifies neglecting the disk self-gravity, as also assumed in (Ward, 2012). Previous works have shown that the convective proto-lunar disk is nearly isothermal vertically due to the large latent heat of condensation of silicates in two-phase regions (Genda and Abe, 2003; Thompson and Stevenson, 1988). Accordingly, we adopt an isothermal vertical structure for the atmosphere with a well-known Gaussian density structure $\rho(z) = \rho(0)\exp(-z^2/H^2)$ and scale height given by $H = \sqrt{2}C_s/\Omega$. Substituting this structure into equation (3) yields a

mass-weighted average height $h_{mass} = \sqrt{2/\pi}\ C_s/\Omega$, and substituting this expression into the second term in equation (2) yields an expression for the liquid-vapor interface pressure:

$$P_{\text{int}} = \frac{1}{\sqrt{2\pi}} f_v \sigma_T C_s \Omega \quad (4)$$

We use this expression to relate the pressure at the liquid-vapor interface to other variables describing the state of the disk locally.

2.2. Radial structure

The disks injected into orbit via giant impacts are generally compact disks, with most of the orbiting mass confined to several planetary radii. For simplicity, here we assume that the surface density profile characterizing the proto-lunar disk scales as ~1/r, as seen in simulations of the standard impact (Canup et al., 2013). High angular momentum impacts (Canup, 2012; Ćuk and Stewart, 2012) tend to create even more compact disks, which may cause identifiable differences in the satellite that would result (Salmon and Canup, 2014). For the purpose of this work, we neglect such differences in radial mass distribution. In order to make a connection between disk process and isotopic observables, we assume that the proto-lunar disk extends from 1-5 Earth radii (R_E) and that the outer disk material (extending from 3-5 R_E) accretes onto the Moon with its isotopic composition expressed in the lunar samples, while the inner disk material (extending from 1-3 R_E) ultimately reaccretes back onto the Earth with its compositional character diluted and essentially erased via mixing into the ~10^2x more massive terrestrial magma ocean. In reality, the process of disk chemical evolution studied here and that of lunar accretion studied elsewhere (Salmon and Canup, 2012) will overlap but any coupling between these processes is beyond the scope of this work and must be subject to future modeling. Here, we restrict the study to evolutionary disk processes that can cause the outer disk to acquire compositional characteristics

183 that are distinct from the inner disk, a distinctness that can be expressed in the composition of
184 silicate Earth and Moon. The initial thermal structure of the disk is taken to be radially isentropic:
185 simulations of impacts find that generated melt-vapor disks are composed of silicate materials that
186 experience similar levels of shock heating (Nakajima and Stevenson, 2014) and are therefore
187 approximately isentropic at the outset. Here, we adopt this isentropic initial state for calculations
188 of the subsequent evolution.
189
190 2.3. Thermodynamic Model
191 We apply a 2-phase, 2-component thermodynamic model recently developed to study liquid-vapor
192 fractionation in the aftermath of the giant impact (Pahlevan et al., 2011) to calculate equilibrium
193 thermodynamic conditions (e.g. T, degree of vaporization) in the proto-lunar disk. The model has
194 been previously described; here we summarize its features and describe its application to the proto-
195 lunar disk. In brief, the silicate liquid is modeled as a binary solution of olivine end-members,
196 $(Fe,Mg)_2SiO_4$, while the silicate vapor is described as a mixture of ideal gases consisting of
197 gaseous species formed upon vaporization of such a liquid: SiO_2, SiO, Si, FeO, Fe, MgO, Mg, O_2,
198 and O. This choice of compositional model is motivated by the fact that the bulk Moon – and
199 therefore the proto-lunar disk – is known to be primarily composed of ferromagnesian silicates
200 (Taylor and Wieczorek, 2014). At each time step in the evolution, we divide the proto-lunar disk
201 into annuli and calculate thermodynamic equilibrium between the liquid layer and overlying vapor
202 atmosphere. Input parameters for equilibrium calculations include the column entropy ranging
203 from highly vaporized to fully condensed states (S=0.530-1.030 kJ/mol.K where mol refers to
204 moles of olivine units or silicon atoms) and column composition (x_c=Fe/Fe+Mg), initially set equal
205 to Earth mantle composition (≈0.1) (Jones and Palme, 2000). Using equations derived from the 2-

phase equilibrium assumption (Pahlevan et al., 2011), as well as the pressure of equilibration (Equation 4), we solve for the interface temperature (T), the column vapor fraction (f_v), the specific entropy (S_L, S_V) and composition (X_L, X_V) of the liquid and atmospheric columns, as well as the partial pressure at the interface of each of nine vapor species (P_i) at each time step and annulus.

2.4. Radial transport

Because of the temperature-dependence of equilibrium partitioning (e.g. Eqn. 9), radial gradients in interface temperature in the disk are expressed as radial gradients in composition of the liquid layer and complementary atmosphere. Given that the disk atmosphere undergoes turbulent convection (Thompson and Stevenson, 1988), the development of compositional gradients will lead to transport of chemical and isotopic species down gradient. Hence, one consequence of an equilibrium fully-stratified (settled liquid) disk model is the development of radial atmospheric compositional gradients that – in concert with a convective, turbulently mixing atmosphere – will lead to net radial transport of chemical and isotopic species. We assume that turbulent convection in the disk atmosphere can be characterized by an eddy diffusivity (Tennekes and Lumley, 1972). In the presence of atmospheric compositional gradients, atmospheric motions will then transport species down gradient in accordance with Fick's law:

$$\vec{J}_i = -\rho_v D_v \vec{\nabla} c_{i,v} \quad (5)$$

where J_i [kg m^{-2} s^{-1}] is the mass flux of an atmospheric constituent *i*, ρ_v is the atmospheric mass density, D_v is the turbulent diffusivity, and $c_{i,v}$ is the atmospheric mass fraction of constituent *i*. In principle, a similar equation could be written for turbulent mixing in the magma layer. However, because of both greater length scales and greater velocity scales associated with atmospheric convection, convective radial transport is expected to be dominated by the atmospheric motions

(Pahlevan and Stevenson, 2007). Accordingly, we consider a liquid layer that is stationary but which rapidly equilibrates with the overlying turbulent atmosphere. We take the divergence of Eqn. (5), combining it with a continuity equation:

$$\frac{\partial\left(\rho_v c_{i,v}\right)}{\partial t} = -\vec{\nabla}\bullet\left(\rho_v D_v \vec{\nabla} c_{i,v}\right) \quad (6)$$

to describe the atmospheric transport. Using the continuity equation here without sources or sinks is valid for species that are neither created nor destroyed in the atmosphere. Atomic abundances can therefore be described in this way, while molecular abundances cannot due to the occurrence of chemical reactions. Note that such an equation is only used to describe changes in the composition of the atmosphere and that compositional changes to the liquid layer arising from liquid-vapor equilibration are treated separately in the numerical model. The reason for this separate treatment is that – unlike signatures that are identical between a silicate liquid and co-existing vapor (e.g. $\Delta^{17}O$ studied in (Pahlevan and Stevenson, 2007)) – here we are considering chemical and isotopic signatures that are distinct between co-existing phases (e.g. $^{30}Si/^{28}Si$, see §2.6). Expecting rapid vertical mixing but rate-limiting radial mixing in the disk, we integrate Eqn. (6) vertically through the convective atmosphere:

$$\sigma_v \frac{\partial c_{i,v}}{\partial t} = -\vec{\nabla}\bullet\left(\sigma_v D_v \vec{\nabla} c_{i,v}\right) \quad (7)$$

where σ_v ($\equiv f_v\sigma_T$) is the atmospheric surface density [kg m^{-2}] and where we have assumed that this parameter has no time-dependence arising from disk turbulence. This assumption reflects the expectation that – while convective motions can drive the transport of species – turbulent convection leads to little or no net mass transfer. Indeed, numerical studies of disks have found that convection does not efficiently transport angular momentum (Lesur and Ogilvie, 2010; Stone and Balbus, 1996), a requirement for net mass transport. This issue is further discussed in §4.1.

Atmospheric surface density does vary in our model due to thermal evolution (i.e. condensation, see §2.5). At each time step, we use Eqn. (7) in cylindrical coordinates to describe changes in atmospheric composition with no net flux boundary conditions, $\partial c/dr(R_E,t) = \partial c/dr(5R_E,t) = 0$. These boundary conditions reflect the simplification of neglecting moonlet formation and satellite-disk interactions in the outer disk (Salmon and Canup, 2012) and turbulent mixing with the silicate vapor atmosphere of Earth in the inner disk (Pahlevan and Stevenson, 2007). Different boundary conditions are possible, but here we make this choice in order to interrogate processes within the proto-lunar disk itself, relegating interactions with its environment to future works.

2.5. Thermal evolution

It is well known that the viscous and thermal evolution of the proto-lunar disk is a closely coupled problem. As first pointed out by (Cameron and Ward, 1976), the material in the proto-lunar disk is susceptible to gravitational instability. These authors later calculated that the viscous evolution timescale for particles undergoing gravitational instability are of order ~1 year (Ward and Cameron, 1978). It was subsequently recognized that such a rapid evolutionary timescale would liberate enough gravitational energy for the material to self-vaporize, violating the original particle assumption (Thompson and Stevenson, 1988). Hence, the idea of a thermally regulated proto-lunar disk arose, whereby the heating due to viscous gravitational energy release would be matched by radiative losses in quasi-steady-state fashion. Accordingly, subsequent works explore coupled solutions to the viscous and thermal evolution (Charnoz and Michaut, 2015; Ward, 2012). Here, we adopt a simplified thermal history in which radiative losses are powered by secular cooling of the disk alone; we do not consider viscous heating. The motivation for, and limitations of, this assumption will be discussed in §4.1.

Treating radiative cooling as a quasistatic process, we can relate the outgoing heat and entropy fluxes using the thermodynamic identity, $dQ = TdS$, where T is the temperature of the radiated photons. Further approximating the radiation as a blackbody, we can write an expression for the entropy per unit area being radiated from both sides of the proto-lunar disk per unit time:

$$dS = 2\sigma_{SB} T_{ph}^{3} dt \quad (8)$$

where σ_{sb} is the Stefan-Boltzmann constant, T_{ph} is the photospheric temperature. We can use this expression to calculate radiative entropy losses from disk annuli as a function of time. Because of vertical convection, we expect the effects of radiative cooling to rapidly propagate down through the column; equivalently, the entire thermal reservoir of the disk can be tapped by radiative losses. At each time step, new values of entropy are derived for each annulus after radiative losses, while radial transport (§2.4) and liquid/atmosphere re-equilibration (§2.3) are calculated using an operator split scheme, i.e. calculating the effects of each process in sequence.

We follow the thermal evolution of the disk from an initial to a final state. Motivated by the impact simulations, we adopt initial thermal states for the proto-lunar disk – measured by the vapor fraction – ranging from mostly (~80%) liquid (Canup, 2004) to mostly (50-95%) vapor (Canup, 2012; Ćuk and Stewart, 2012). For final states, because we are interested in articulating expected compositions of the outer disk material, and because atmospheric transport is expected to dominate the radial transport over liquid-layer convection (§2.4), once the vapor in the outer disk (3-5 R_E) has nearly fully condensed ($f_v < 0.01$), the composition of the liquid is considered frozen-in, to be later expressed in the isotopic composition of the silicate Moon, i.e. of lunar samples. Hence, we consider the evolution of the disk until the outer disk has fully condensed. In addition to neglecting

297 viscous heating, we do not consider turbulent radial transport of entropy and heat in the
298 atmosphere, or other possible triggers of compositional freeze-in, e.g. disk fragmentation into
299 moonlets, but discuss variations in disk models in §4.2 and §4.3.
300
301 2.6. Silicon isotopes as tracers
302 We choose to study the behavior of silicon isotopes as tracers for several reasons. First, it is known
303 that at sufficiently high temperature, equilibrium isotopic differences between co-existing phases
304 approach zero (Urey, 1947) and that small but significant isotopic fractionation is only possible at
305 high temperature where there are significant differences in bonding environment between the
306 phases present for the element under consideration. Silicon, for example, exists as SiO_4^{-4} in silicate
307 melts and predominantly as SiO in co-existing vapors (Visscher and Fegley, 2013), permitting
308 large liquid-vapor isotopic fractionation (~0.5 per mil in $^{30}Si/^{28}Si$) in the high-temperature
309 environment (~3,000-4,000 K) encountered during lunar origin (Pahlevan et al., 2011). Second,
310 unlike magnesium, iron, and oxygen, which significantly reside in multiple species in silicate
311 vapors, SiO dominates the vapor speciation of silicon (e.g. over SiO_2 and Si) for the full range of
312 conditions encountered in the proto-lunar disk (Visscher and Fegley, 2013). Because of such
313 simple vapor speciation, even a two-component thermodynamic model (see §2.3) accurately
314 captures the speciation behavior for silicon in the actual proto-lunar disk, a requirement for
315 accurately articulating predictions of isotopic fractionation in scenarios of evolution. Finally, to
316 forge a connection with observables, we require an element whose isotopic composition in the
317 bulk silicate Earth and Moon are precisely known. Because the bonding environment for silicon
318 in silicate melts and co-existing crystals are rather similar (Huang et al., 2014; Méheut et al., 2009),
319 the silicon isotopic variations that arise due to liquid-vapor fractionation are not encountered

during ordinary (i.e. crystal-liquid) petrologic processes (Fitoussi et al., 2009; Savage et al., 2009; Zambardi et al., 2013). Accordingly, the isotopic composition of samples reflects the process of liquid-vapor fractionation in the proto-lunar disk but not the subsequent crystal-liquid geologic fractionations. Hence, the isotopic composition of the silicate Earth and Moon can be derived from measurements on samples and are known to high precision, permitting comparison of the observations with predictions of the post giant-impact evolution (Armytage et al., 2012; Pahlevan, 2014).

Silicon isotopes are integrated as passive tracers into the model. At each time step, liquid-vapor equilibrium at each annulus is characterized by a temperature, T (see §2.3). Because the isotopic fractionation is only a function of temperature in this low-pressure (<1GPa) system, we can calculate the partitioning of Si isotopes between the silicate liquid and vapor as:

$$\Delta_{L-V} = 5 \times (10^3 / T)^2 \ \ per\ mil \tag{9}$$

$$\delta_C = F_V^{Si} \delta_V + (1 - F_V^{Si}) \delta_L \tag{10}$$

where $\Delta_{L\text{-}V}=\delta_L-\delta_V$ is the part per thousand difference of the $^{30}Si/^{28}Si$ between the liquid and vapor, as previously calculated using standard procedures (Pahlevan et al., 2011) and δ_L, δ_V, δ_C represent the isotopic compositions of the liquid layer, the vapor atmosphere and the entire column (liquid layer plus atmosphere). We set the initial disk composition $\delta_C(r,0)$ to zero for reference. In this way, one can calculate the radial isotopic structure of the proto-lunar disk atmosphere and liquid layer, given a radial disk composition, $\delta c(r,t)$ and temperature structure, $T(r,t)$. Two features of the isotopic partitioning are notable. First, $\Delta_{L\text{-}V}$ is positive, such that the heavier isotopes of silicon will concentrate into the silicate liquids. Second, the temperature dependence of the fractionation guarantees spatial variations in the liquid-vapor partitioning throughout the proto-lunar disk. In

343 particular, the radial gradient in equilibration temperature will be expressed – through equilibrium
344 partitioning (Eqn. 9) – as silicon isotopic gradients in the atmosphere and liquid layer. Once this
345 equilibrium state is calculated, we propagate the evolution forward by calculating the radial
346 isotopic transport via Eqn. (7), where $c_{i,v}$ now represents δ_V. After calculating radial transport, we
347 permit the atmosphere – now out of equilibrium with the underlying liquid layer – to re-equilibrate,
348 thereby changing the composition of the lunar-forming liquid. In this way, turbulent motions in
349 the convective vapor atmosphere alone can change the isotopic composition of the nominally
350 stationary Moon-forming liquid. In the case of silicon, such isotopic redistribution tends to
351 concentrate the heavy isotopes in the outer (i.e. Moon-forming) regions of the disk.
352
353 **3. Results**
354 3.1. Thermal state and history
355 Because of the weak (logarithmic) dependence of the specific entropy of ideal gases with pressure,
356 the initial isentropic state of the proto-lunar disk translates to a radially ~constant vapor fraction
357 initially (Figure 1a). Because of high latent heat of condensation and high vapor fractions (~tens
358 of percent), the secular cooling heat budget of the proto-lunar disk is dominated by latent heat of
359 condensation, with minor contributions from sensible heat ($c_p\Delta T$). Hence, unlike the post-impact
360 atmosphere of Earth which is thermally buffered from below, secular cooling of the proto-lunar
361 disk in the absence of viscous heating is rapid. Because of an outwardly decreasing surface density
362 profile, the disk first cools at large distances with a condensation front that propagates inwards on
363 a timescale of years (Figure 1a).
364

365 The temperature structure of the disk has several notable features. First, even at the outset of the
366 evolution, an isentropic disk is characterized by a significant radial temperature gradient, as also
367 observed in (Nakajima and Stevenson, 2014). Second, because of more rapid cooling in the outer
368 disk, the radial T-gradient of the disk steepens with time, ranging from 125-350 K/R_E (Figure 1b).
369 The existence of such a radial temperature gradient is expected to be a universal feature of any
370 proto-lunar disk model and plays a central role in the evolution of isotopic signatures here studied.
371
372 3.2. Major element chemical fractionation
373 The 2-component [$(Fe,Mg)_2SiO_4$] thermodynamic model adopted has one variable for chemical
374 composition, x_{Fe}(≡Fe/Fe+Mg), rendering possible studies of chemical fractionation. Accordingly,
375 we track the x_{Fe} of the liquid, vapor, and total column in the proto-lunar disk during the evolution.
376 As has been experimentally determined, fayalite (Fe_2SiO_4) has a higher vapor pressure than
377 forsterite (Mg_2SiO_4) at identical temperature (Nagahara et al., 1994), a behavior clearly expressed
378 in the proto-lunar disk: the vapor atmosphere is enriched in FeO (x_{Fe}=0.12-0.35), while the liquid
379 layer is MgO-rich (x_{Fe}=0.02-0.06), relative to the composition of the column as a whole (x_{Fe}=0.1,
380 Figure 2a). Moreover, due to the temperature and pressure gradients in the disk, even an initial
381 radial chemical homogeneity will – through equilibrium partitioning – result in radial chemical
382 gradients in liquid and atmospheric reservoirs. An increasing iron oxide content of the vapor
383 atmosphere with radius (Figure 2a) implies an inward turbulent transport of iron in the atmosphere
384 arising from convective turbulence. Through liquid-vapor re-equilibration, atmospheric transport
385 of species also leads to the development of chemical gradients in the lunar-forming liquid. In this
386 way, turbulent transport can be expected to redistribute chemical species in the proto-lunar disk.
387

Two features of turbulent chemical transport are notable: (i) the outer disk material from which the Moon forms is modestly depleted in iron-rich silicates relative to the inner disk, which falls back onto Earth (Figure 2b). The sign of this fractionation can be understood as follows: as the outermost disk condenses, it becomes increasingly iron-rich (Figure 2a), such that turbulent mixing with the hotter, more highly vaporized inner disk depletes FeO from the lunar-forming material, (ii) the magnitude of chemical fractionation is modestly dependent on initial disk vapor fraction (Figure 2b). This result can be understood since higher vapor fractions are associated with longer secular cooling timescales (§3.1), permitting the chemical redistribution to proceed longer, and since it implies a greater atmospheric mass, in which transport occurs, relative to the mass of the melt layer, permitting more efficient turbulent transport and steeper chemical gradients to develop per unit time. Unsurprisingly, more vigorous turbulence results in greater chemical redistribution. For the major elements here considered, this effect is small but non-negligible: for the range of initial vapor fractions and turbulent diffusivities considered for the proto-lunar disk, the resulting depletion in outer disk Fe/Fe+Mg is < 2x (Figure 3). Hence, impact models that begin with an Earth-mantle-like disk (Canup, 2012; Ćuk and Stewart, 2012) cannot generate an FeO-enriched silicate Moon (Jones and Palme, 2000; Sakai et al., 2014) via turbulent redistribution: some other process is required. Nevertheless, due to uncertainties in both the initial Fe/Fe+Mg in the proto-lunar disk as well as in the lunar bulk chemical composition, modest chemical fractionation in the proto-lunar disk is difficult to rule out using major elements. We conclude that the major element composition of the Moon places modest constraints on chemical fractionation processes in the proto-lunar disk.

3.3. Silicon isotope fractionation

411 Equilibrium silicon isotopic fractionation is significant, resulting in a ~0.4-0.5 per mil difference
412 in the $^{30}Si/^{28}Si$ of silicate liquids and vapors at the temperatures prevailing in the proto-lunar disk
413 (Figure 4a). As discussed in §2.6, the proto-lunar liquid concentrates the heavy isotopes of silicon
414 while the complementary vapor atmosphere is isotopically light, with the difference between the
415 two reservoirs increasing with increasing radius, due to the negative radial temperature gradient
416 (Figure 2b) and equilibrium partitioning law (Equation 9), which dictates enhanced fractionation
417 at lower temperatures. The resulting composition of the atmosphere exhibits greater isotopic
418 lightness with increasing radial distance and implies an inward transport of light silicon isotopes
419 accompanying turbulent convection in the atmosphere. Liquid-vapor equilibration transmits this
420 signal to the proto-lunar liquid and the process continues until the proto-lunar disk has condensed
421 and the isotopic structure has frozen in. As with chemical fractionation (§3.2), steeper gradients
422 are generated from hotter initial states (Figure 4b), the reasons being two-fold: longer cooling
423 timescales and greater atmospheric masses cause greater transport and redistribution during the
424 cooling history as a by-product of turbulent convection.
425
426 The magnitude of the silicon isotope fractionation is large relative to the precision with which the
427 composition of terrestrial and lunar reservoirs is measured, permitting the development of a new
428 stable isotopic tracer for the evolution of the proto-lunar disk. As in the case of chemical
429 fractionation (§3.2), both more vigorous turbulence (higher α) and hotter initial thermal states
430 result in greater isotopic fractionation between the outer (Moon-forming) and inner (Earth-bound)
431 proto-lunar disk (Figure 5). For nominal values of turbulent diffusivity ($\alpha=3x10^{-3}$), even modestly
432 vaporized proto-lunar disks (f_v~0.2-0.4) can imprint measurable mass-dependent signatures onto
433 the lunar forming material ($\delta^{30}Si_M$=0.05-0.1‰ – Figure 5). An Earth-Moon isotopic offset of this

434 magnitude can be excluded by existing observations (Armytage et al., 2012; Fitoussi and Bourdon,
435 2012). Possible interpretations of the data in light of the model results are discussed in §4.4.
436
437 **4. Discussion**
438 We have described a coupled thermochemical model for the evolution of the proto-lunar disk with
439 the goal of forging a link between the stable isotopic composition of the lunar-forming material
440 and the parameters governing lunar disk evolution. Here, we discuss several simplifying features
441 of the adopted disk model, compare with other disk models discussed in the literature (§4.1-4.3),
442 and then consider the general conclusions that can be drawn about the evolution of the proto-lunar
443 disk using the model with constraints provided by the stable isotopic data (§4.4).
444
445 4.1. Viscous evolution
446 The model we have described neglects the viscous redistribution of mass and angular momentum
447 and the attendant gravitational energy release. Including viscous evolution into the disk model
448 would have several effects: (1) thermal: due to the depth of the terrestrial gravity well, significant
449 viscous spreading has significant thermal consequences; where viscous heating takes place, it can
450 easily dominate the heat budget of the melt-vapor column. For example, (Ward, 2012) described
451 a disk model characterized by a stratified melt-vapor structure with a viscous melt layer and an
452 inviscid atmosphere, and derived a cooling timescale for the proto-lunar disk of ~250 years, to be
453 compared with a cooling timescale of ~2 years for a f_v~0.2 disk powered by secular cooling alone
454 (§3.1). Hence, one consequence for the purely secular cooling powered disk model here described
455 is that the lifetime – and the magnitude of chemical and isotopic redistribution calculated for the
456 proto-lunar disk – are lower limits. The lifetime and degree of chemical fractionation is expected

to be greater in a model such as that described in (Ward, 2012), (2) transport/redistribution: viscous dissipation causes outward (inward) transport of angular momentum (mass) and causes material to spread radially, a flow that competes with turbulent mixing (Stevenson, 1990). Hence, by neglecting the viscous evolution, we implicitly only consider diffusive ($D/\nu \geq 1$) evolutionary regimes. We have focused on this regime because it is in this regime in which extensive turbulent mixing may take place (Pahlevan and Stevenson, 2007). However, even if a partially vaporized disk is initially in the diffusive regime, it is possible that – as the disk condenses – it transitions to the viscous regime ($D/\nu \leq 1$) where radial mixing becomes inefficient. The calculations here presented only apply to redistribution in the diffusive regime.

4.2. Turbulent heat and entropy transport

We have considered turbulent transport in the presence of compositional gradients, but neglected the equivalent transport of heat in the presence of atmospheric entropy gradients. It is known that – in the presence of radial entropy gradients – a disk instability may arise at the expense of the entropy gradient ("radial convection") and thereby radially transport heat and entropy (Klahr and Bodenheimer, 2003; Lesur and Papaloizou, 2010). In the proto-lunar disk, such a radial entropy gradient may arise via preferential cooling or vertical phase separation of droplets ("rainout") in adjacent annuli of the proto-lunar disk. This process would have consequences for the calculations here presented: (1) thermal: since heat transport is outward, to the extent that this process takes place, it prolongs the thermal history and accentuates the chemical/isotopic signals that arise, and (2) compositional: since the effective gravity in the near-Keplerian disk is inwards, this process would also exchange vapor-rich (isotopically light) atmospheric parcels with more liquid-rich (isotopically heavy) parcels radially and may therefore moderate the magnitude of radial transport

here calculated and soften the constraint here described. However, we see no reason to suppose that this effect would precisely cancel the isotopic fractionation based on the radial temperature gradient calculated in this work. In the absence of such a reason, the possibility of a fortuitous cancellation of two competing effects is considered unlikely. This issue needs to be investigated further.

4.3. Criterion for compositional freeze-in

While adopting initial conditions for disk evolution from the output of giant impact simulations is straightforward, selecting a criterion for the cessation of disk evolution is less certain. Here, we have considered a disk with chemical and isotopic redistribution but no net mass transport and no fragmentation. In such a model, the condensation of the vapor atmosphere can be expected to halt radial redistribution because the turbulent atmosphere is the agent that causes transport. However, other criteria for compositional freezing of the disk are possible. (Canup et al., 2015) considered a settled disk with a viscous liquid-rich midplane layer. In analogy with particle disks, the midplane liquid layer was assumed to undergo gravitational instability and fragmentation to form moonlets beyond the classical Roche radius at 2.9 R_E defined by lunar-density condensates. (Thompson and Stevenson, 1988) instead considered a disk model in which a single vertical isentrope characterized convective columns from the midplane up to the rarified regions where the disk atmosphere is optically thin and radiative. In such a picture, radiative cooling in disk patches is balanced by gravitational energy release until the material spreads to radii where this equality can no longer be satisfied, at which point the patch instabilities lead to collapse and moonlet formation and the composition of the moonlets is determined by the composition of the collapsing disk fragment with constituent droplets and vapor. Regardless of the precise criterion for compositional freeze-

503 in for disk patches, it is clear that the liquid composition is effectively frozen-in once the vapor
504 atmosphere condenses. Moreover, satellite-disk interaction may also be important (Salmon and
505 Canup, 2012) but its coupling with the disk evolution must be relegated to future works.
506
507 4.4. Consequences for disk evolution and equilibration
508 We do not know – a priori – how the proto-lunar disk evolved. Here, we have considered a disk
509 model in which the liquid largely settles out into a liquid-rich layer that rapidly equilibrates with
510 the overlying atmosphere, with the turbulent diffusivity in the vapor atmosphere operating on a
511 shorter timescale than viscous dissipation in either the atmosphere (Carballido et al., 2016) or the
512 melt-rich layer (Ward, 2012). This is the same settling and transport regime originally envisaged
513 in the equilibration hypothesis (Pahlevan and Stevenson, 2007) and therefore provides constraints
514 on an evolutionary scenario of this kind. We have shown that in such a picture the proto-lunar disk
515 is expected to generate isotopic gradients that would be expressed as differences in the composition
516 of the silicate Earth and Moon. Such an Earth-Moon isotopic offset is not observed to a precision
517 of 30 ppm in the case of the silicon ($^{30}Si/^{28}Si$) (Armytage et al., 2012; Fitoussi and Bourdon, 2012).
518 In the light of the isotopic observations, the results of the modeling can be interpreted in four ways:
519 (1) imperfect settling: the proto-lunar liquid may fail to settle into a liquid-rich layer with a
520 separately convective atmosphere and instead, exchange between the midplane and vapor
521 atmosphere may be advective (e.g. convective overshoot), as also described in (Thompson and
522 Stevenson, 1988). In such a scenario, equilibration with the Earth would involve both a vapor
523 atmosphere as well as the suspended liquid droplets, and one would expect isotopic homogeneity
524 in the Earth-Moon system for all elements irrespective of volatility, (2) liquid-vapor equilibration:
525 we have assumed that liquid-vapor equilibration in this system is rapid relative to transport

timescales in the problem. While the vigor of convective motion makes this possible, the timescale for liquid-vapor equilibration may depend on foam-physics at the liquid-vapor interface and is therefore difficult to quantify. Hence, one interpretation of the silicon isotopic data is that the liquid and vapor in the proto-lunar disk underwent phase separation into two distinct layers but did not experience continuous and rapid chemical re-equilibration. While very large depletions of volatile elements in the lunar material suggest that nearly all proto-lunar liquid equilibrated with some vapor, a timescale for liquid-vapor equilibration comparable to the evolutionary timescale cannot be ruled out, (3) other transport regimes: we have here restricted the discussion to transport regimes in which the total diffusivity is greater than the total viscosity ("the diffusive regime") such that mixing can outcompete disk spreading and homogenize the vapor atmosphere on a rapid timescale. This regime may be appropriate for a disk whose dominant instability is the convective instability, because convection in disks is known to produce turbulent mixing but weak angular momentum transport (Lesur and Ogilvie, 2010; Stone and Balbus, 1996). However, there exist other instabilities, e.g. the gravitational instability, that may entail different mixing and transport properties. Hence, it is also possible that the disk spent part of its evolution in the viscous regime not subject to the diffusive redistribution process here calculated., (4) high-temperature silicate thermodynamics: it is possible that a binary olivine thermodynamics does not accurately capture the vaporization behavior of silicon in the proto-lunar disk on which the modeling results are based. In particular, olivine is known to vaporize congruently (Nagahara et al., 1994) such that the degree of silicate vaporization is and silicon vaporization are equivalent in an olivine thermodynamics. A more complex multi-component model need not display this behavior, rending silicon isotopes highly sensitive to the evolution of the proto-lunar disk for only a range of vapor fractions. The degree to which olivine thermodynamics accurately captures the vaporization behavior of any

given element in the proto-lunar disk can be determined by development of more complex models of multi-component silicate melts at the temperatures (T=3,000-4,000 K) of relevance.

5. Conclusions

Recent isotopic observations on lunar and terrestrial samples strongly suggest that the lunar material is derived from the silicate Earth. While the disk stage of lunar evolution has been invoked to explain several features of the Earth-Moon system, including the high-precision isotopic homogeneity, a quantitative and observationally constrained description of proto-lunar disk evolution is lacking. Despite uncertainty in the initial thermal state, the settling and transport regimes, and the degree of thermal and chemical coupling to the post-impact Earth, it is well established that the proto-lunar disk experiences a two-phase (liquid-vapor) evolution. Here, we have developed a thermochemical scenario of disk evolution incorporating silicon isotopes as passive tracers. Our results demonstrate that silicon isotopic fractionation in the proto-lunar disk can be significant relative to the precision of existing measurements, yielding a new quantitative constraint on disk evolution. The principal conclusion of the model is that a "settled" proto-lunar disk in the diffusive regime would have developed isotopic offsets in the silicate EM system that are not observed. Hence, it is possible to use silicon isotopes to set constraints on Earth-disk equilibration: if system-wide turbulent mixing of the Earth-Moon system took place, it must have involved advective mixing of the proto-lunar liquid and the vapor atmosphere. Whether other disk evolutionary scenarios – including highly vaporized disks generated by recently explored impacts – can be reconciled with the silicon isotopic homogeneity of the EM system must be the subject of future studies. These results open a new quantitative window into the energetic aftermath of the Moon-forming giant impact.

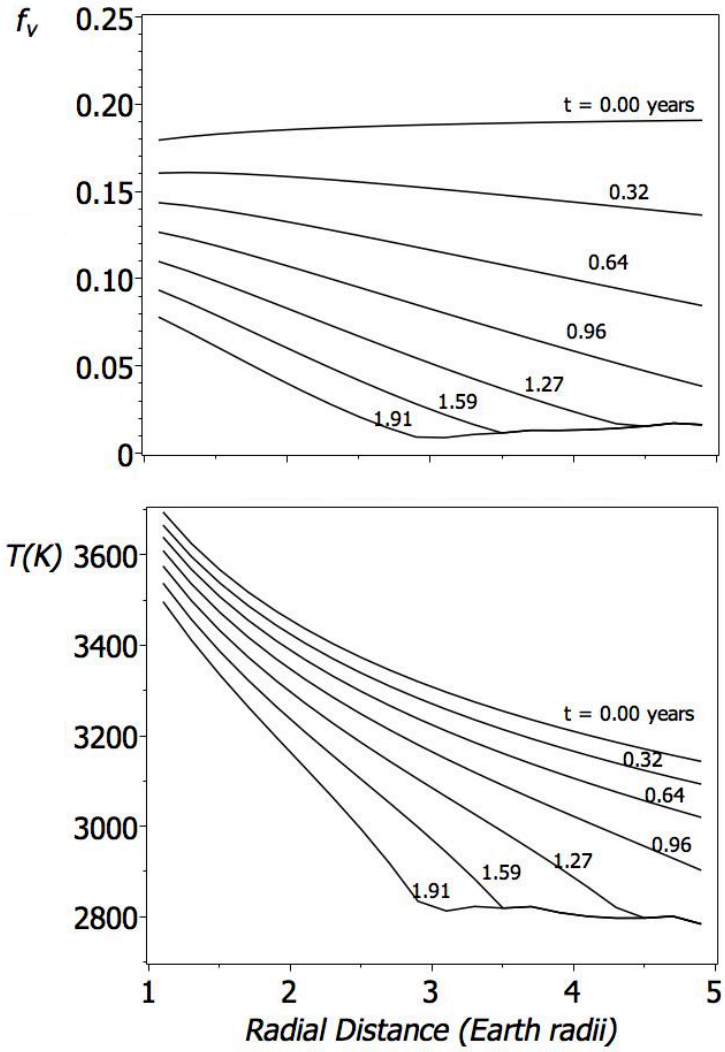

Figure 1. Disk thermal state and evolution. (a) Disk vapor fraction (atmospheric mass / total disk column mass) versus radial distance. This cooling history corresponds to an initial condition (f_v~0.2) generated via the "standard" impact. The simulations are halted at f_v~0.01 for numerical reasons. (b) Equilibration temperatures at the liquid-vapor interface versus radial distance. Note that, even in an initially isentropic disk, the disk is characterized by a radial temperature gradient due to the radial pressure gradient arising from e.g. radial surface density gradients in the disk, and cooling of the disk only accentuates a pre-existing T-gradients.

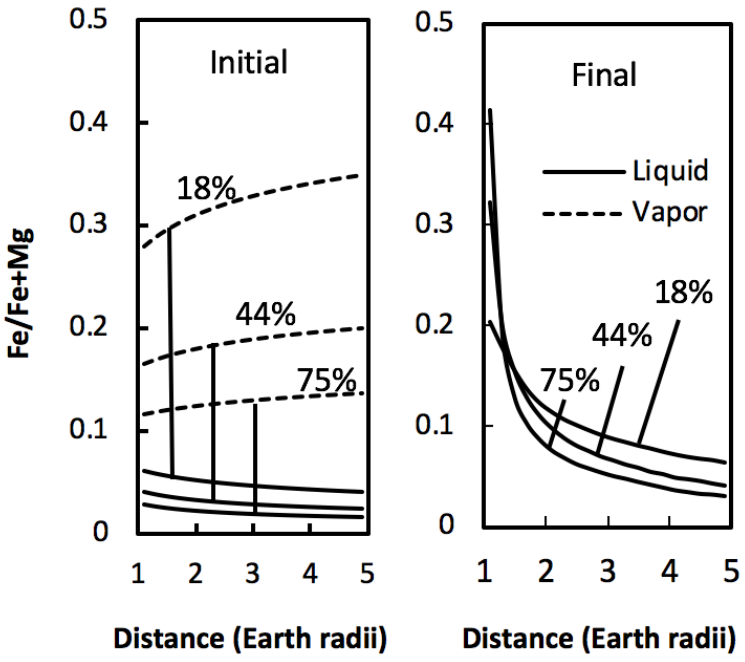

Figure 2. Fe/Mg redistribution in the proto-lunar disk. (a) Initial liquid-vapor partitioning in a disk with bulk x_{Fe}(Fe/Fe+Mg)=0.1. The percentage labels on curves correspond to initial disk vapor fraction. (b) Final compositional structure of the disk when the vapor has condensed and the liquid composition has frozen in. The vigor of turbulence in these simulations is $\alpha=3\text{x}10^{-3}$.

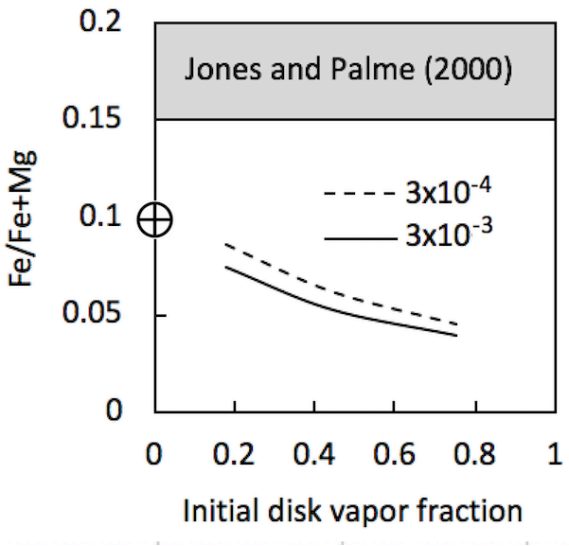

Figure 3. Summary of major element redistribution calculations. The curves represent final Fe/Fe+Mg of the outer (i.e. Moon-forming) disk after condensation versus the initial thermal state of the proto-lunar disk for two different values of the turbulent α parameter. Initial major element composition (i.e. Fe/Fe+Mg) of the disk is assumed to be the same in all cases ($\equiv$0.1), corresponding to a bulk silicate Earth initial composition. Non-zero turbulent diffusivity leads to redistribution of chemical species. While modest Fe/Fe+Mg variations can arise in the proto-lunar disk, the fractionation is of the wrong sign to produce the FeO enrichment of the bulk Moon, indicated by the shaded region).

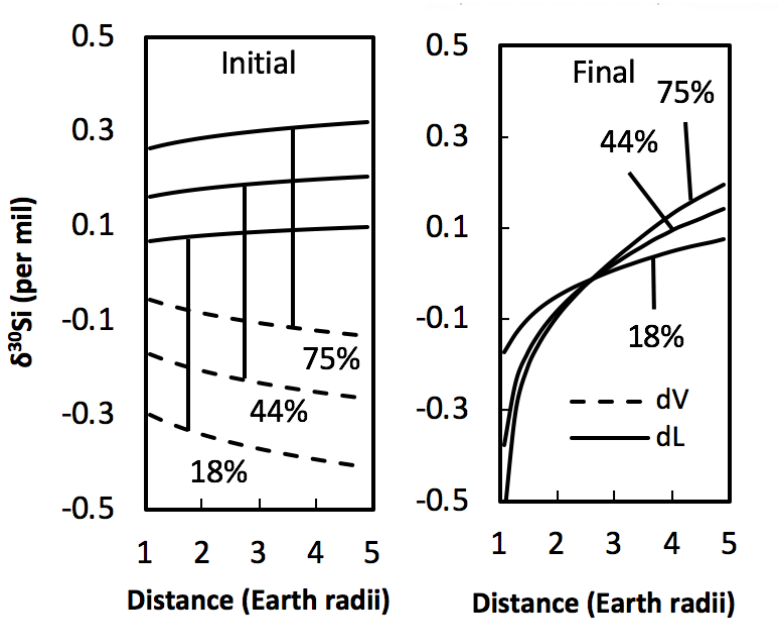

Figure 4. Silicon isotopic fractionation in the proto-lunar disk. (a) The initial radial isotopic structure of the proto-lunar disk atmosphere and liquid layer, with disks assumed to have a radially uniform initial composition set to zero for reference ($\delta^{30}Si=0$). The number labels on the curves correspond to the initial disk vapor fraction. Equilibrium partitioning leads to a liquid layer that is isotopically heavy with a complementary isotopically light atmosphere. (b) Final isotopic structure of the disk at the end of the thermal history when the vapor has condensed and the liquid composition has frozen in. The increasing isotopic lightness of the vapor atmosphere with radius implies in an inward transport of light isotopes whose magnitude depends on the disk initial vapor fraction.

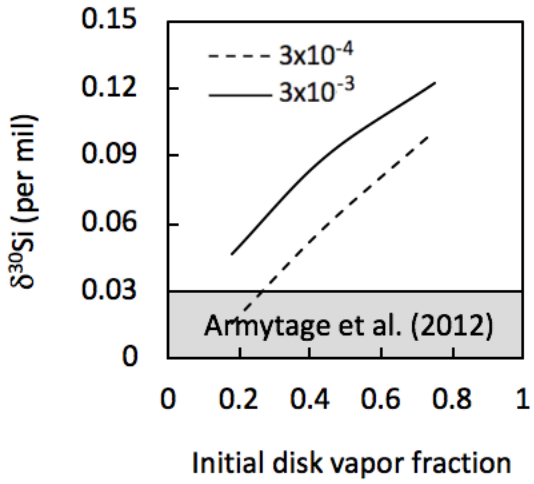

Figure 5. Summary of silicon isotopic redistribution in the proto-lunar disk. The average isotopic composition of the outer Moon-forming disk (3-5R_E) is plotted as a function of the initial vapor fraction for two different values of the turbulent α parameter. The initial composition of the disk ($\delta^{30}Si$) is set to zero in these calculations for reference. In the absence of radial diffusivity, the final and initial composition of the outer disk would be identical, but for even modest levels of turbulence, measurable isotopic differences between the inner and outer disk can evolve. Measurements on terrestrial and lunar samples observe no $\delta^{30}Si$ difference between the Earth and Moon ($\Delta^{30}Si\text{-}EM=\delta^{30}Si_E-\delta^{30}Si_M$) at a precision of < 0.03 per mil (Armytage et al., 2012; Fitoussi and Bourdon, 2012). Possible interpretations are discussed in §4.

References

Armytage, R.M.G., Georg, R.B., Williams, H.M., Halliday, A.N., 2012. Silicon isotopes in lunar rocks: implications for the Moon's formation and early history of the Earth. Geochimica Et Cosmochimica Acta, In Press.

Atobe, K., Ida, S., 2007. Obliquity evolution of extrasolar terrestrial planets. Icarus 188, 1-17.

Cameron, A.G.W., Ward, W.R., 1976. The origin of the Moon. Lunar Sci. 7, 120-122.

Canup, R.M., 2004. Simulations of a late lunar-forming impact. Icarus 168, 433-456.

Canup, R.M., 2008. Lunar-forming collisions with pre-impact rotation. Icarus 196, 518-538.

Canup, R.M., 2012. Forming a Moon with an Earth-like Composition via a Giant Impact. Science 338, 1052-1055.

Canup, R.M., Asphaug, E., 2001. Origin of the Moon in a giant impact near the end of the Earth's formation. Nature 412, 708-712.

Canup, R.M., Barr, A.C., Crawford, D.A., 2013. Lunar-forming impacts: High-resolution SPH and AMR-CTH simulations. Icarus 222, 200-219.

Canup, R.M., Visscher, C., Salmon, J., Fegley Jr, B., 2015. Lunar volatile depletion due to incomplete accretion within an impact-generated disk. Nature Geosci 8, 918-921.

Carballido, A., Desch, S.J., Taylor, G.J., 2016. Magneto-rotational instability in the protolunar disk. Icarus 268, 89-101.

Charnoz, S., Michaut, C., 2015. Evolution of the protolunar disk: Dynamics, cooling timescale and implantation of volatiles onto the Earth. Icarus 260, 440-463.

Ćuk, M., Hamilton, D.P., Lock, S.J., Stewart, S.T., 2016. Tidal evolution of the Moon from a high-obliquity, high-angular-momentum Earth. Nature 539, 402-406.

Ćuk, M., Stewart, S.T., 2012. Making the Moon from a Fast-Spinning Earth: A Giant Impact Followed by Resonant Despinning. Science 338, 1047-1052.

Fitoussi, C., Bourdon, B., 2012. Silicon Isotope Evidence Against an Enstatite Chondrite Earth. Science 335, 1477-1480.

Fitoussi, C., Bourdon, B., Kleine, T., Oberli, F., Reynolds, B.C., 2009. Si isotope systematics of meteorites and terrestrial peridotites: implications for Mg/Si fractionation in the solar nebula and for Si in the Earth's core. Earth and Planetary Science Letters 287, 77-85.

Genda, H., Abe, Y., 2003. Modification of a proto-lunar disk by hydrodynamic escape of silicate vapor. Earth Planets and Space 55, 53-57.

Halliday, A.N., 2012. The Origin of the Moon. Science 338, 1040-1041.

Hartmann, W.K., Davis, D.R., 1975. Satellite-sized planetesimals and lunar origin. Icarus 24, 504-515.

Holton, J.R., 1992. An Introduction to Dynamic Meteorology. Academic Press, San Diego.

607 Huang, F., Wu, Z., Huang, S., Wu, F., 2014. First-principles calculations of equilibrium silicon
608 isotope fractionation among mantle minerals. Geochimica et Cosmochimica Acta 140, 509-520.
609 Jones, J.H., Palme, H., 2000. Geochemical constraints on the origin of the Earth and Moon, in:
610 Righter, K., Canup, R.M. (Eds.), Origin of the Earth and Moon. University of Arizona Press, Tucson,
611 AZ, pp. 197-216.
612 Klahr, H.H., Bodenheimer, P., 2003. Turbulence in Accretion Disks: Vorticity Generation and
613 Angular Momentum Transport via the Global Baroclinic Instability. The Astrophysical Journal 582,
614 869.
615 Kruijer, T.S., Kleine, T., Fischer-Godde, M., Sprung, P., 2015. Lunar tungsten isotopic evidence for
616 the late veneer. Nature 520, 534-537.
617 Lesur, G., Ogilvie, G.I., 2010. On the angular momentum transport due to vertical convection in
618 accretion discs. Monthly Notices of the Royal Astronomical Society: Letters 404, L64-L68.
619 Lesur, G., Papaloizou, J.C., 2010. The subcritical baroclinic instability in local accretion disc
620 models. Astronomy & Astrophysics 513, A60.
621 Machida, R., Abe, Y., 2004. The evolution of an impact-generated partially vaporized
622 circumplanetary disk. Astrophysical Journal 617, 633-644.
623 Méheut, M., Lazzeri, M., Balan, E., Mauri, F., 2009. Structural control over equilibrium silicon and
624 oxygen isotopic fractionation: A first-principles density-functional theory study. Chemical
625 Geology 258, 28-37.
626 Nagahara, H., Kushiro, I., Mysen, B.O., 1994. Evaporation of Olivine - Low-Pressure Phase-
627 Relations of the Olivine System and Its Implication for the Origin of Chondritic Components in the
628 Solar Nebula. Geochimica Et Cosmochimica Acta 58, 1951-1963.
629 Nakajima, M., Stevenson, D.J., 2014. Investigation of the initial state of the Moon-forming disk:
630 Bridging SPH Cross Mark simulations and hydrostatic models. Icarus 233, 259-267.
631 Pahlevan, K., 2014. Isotopes as tracers of the sources of the lunar material and processes of lunar
632 origin. Philosophical Transactions of the Royal Society a-Mathematical Physical and Engineering
633 Sciences 372.
634 Pahlevan, K., Morbidelli, A., 2015. Collisionless encounters and the origin of the lunar inclination.
635 Nature 527, 492-494.
636 Pahlevan, K., Stevenson, D.J., 2007. Equilibration in the aftermath of the lunar-forming giant
637 impact. Earth and Planetary Science Letters 262, 438-449.
638 Pahlevan, K., Stevenson, D.J., Eiler, J.M., 2011. Chemical fractionation in the silicate vapor
639 atmosphere of the Earth. Earth and Planetary Science Letters 301, 433-443.
640 Reufer, A., Meier, M.M.M., Benz, W., Wieler, R., 2012. A hit-and-run giant impact scenario. Icarus
641 221, 296-299.
642 Sakai, R., Nagahara, H., Ozawa, K., Tachibana, S., 2014. Composition of the lunar magma ocean
643 constrained by the conditions for the crust formation. Icarus 229, 45-56.
644 Salmon, J., Canup, R.M., 2012. Lunar Accretion from a Roche-Interior Fluid Disk. Astrophysical
645 Journal 760.
646 Salmon, J., Canup, R.M., 2014. Accretion of the Moon from non-canonical discs. Philosophical
647 Transactions of the Royal Society a-Mathematical Physical and Engineering Sciences 372.
648 Savage, P.S., Georg, R.B., Williams, H.M., Halliday, A.N., 2009. Uniform silicon isotopes in the
649 depleted mantle and no melt-induced fractionation. Geochimica Et Cosmochimica Acta 73,
650 A1162-A1162.

651 Schiller, M., Bizzarro, M., Fernandes, V.A., 2018. Isotopic evolution of the protoplanetary disk and
652 the building blocks of Earth and the Moon. Nature 555, 507.
653 Stevenson, D.J., 1990. Chemical Heterogeneity and Imperfect Mixing in the Solar Nebula.
654 Astrophysical Journal 348, 730-737.
655 Stone, J.M., Balbus, S.A., 1996. Angular momentum transport in accretion disks via convection.
656 Astrophysical Journal 464, 364-372.
657 Taylor, G.J., Wieczorek, M., 2014. Lunar bulk chemical composition: a post-Gravity Recovery and
658 Interior Laboratory reassessment. Philosophical Transactions of the Royal Society a-
659 Mathematical Physical and Engineering Sciences 372.
660 Tennekes, H., Lumley, J.L., 1972. A First Course on Turbulence. The MIT Press, Cambridge,
661 Massachusetts.
662 Thompson, C., Stevenson, D.J., 1988. Gravitational-Instability in 2-Phase Disks and the Origin of
663 the Moon. Astrophysical Journal 333, 452-481.
664 Tian, Z., Wisdom, J., Elkins-Tanton, L., 2017. Coupled orbital-thermal evolution of the early Earth-
665 Moon system with a fast-spinning Earth. Icarus 281, 90-102.
666 Touboul, M., Puchtel, I.S., Walker, R.J., 2015. Tungsten isotopic evidence for disproportional late
667 accretion to the Earth and Moon. Nature 520, 530-533.
668 Touma, J., Wisdom, J., 1998. Resonances in the early evolution of the earth-moon system.
669 Astronomical Journal 115, 1653-1663.
670 Urey, H.C., 1947. The Thermodynamic Properties of Isotopic Substances. Journal of the Chemical
671 Society, 562-581.
672 Visscher, C., Fegley, B., 2013. Chemistry of Impact-Generated Silicate Melt-Vapor Debris Disks.
673 Astrophysical Journal Letters 767.
674 Ward, W.R., 2012. On the Vertical Structure of the Protolunar Disk. Astrophysical Journal 744.
675 Ward, W.R., Cameron, A.G.W., 1978. Disc Evolution Within the Roche Limit, Lunar and Planetary
676 Science Conference IX, Houston, Texas.
677 Ward, W.R., Canup, R.M., 2000. Origin of the Moon's orbital inclination from resonant disk
678 interactions. Nature 403, 741-743.
679 Wisdom, J., Tian, Z.L., 2015. Early evolution of the Earth-Moon system with a fast-spinning Earth.
680 Icarus 256, 138-146.
681 Young, E.D., Kohl, I.E., Warren, P.H., Rubie, D.C., Jacobson, S.A., Morbidelli, A., 2016. Oxygen
682 isotopic evidence for vigorous mixing during the Moon-forming giant impact. Science 351, 493-
683 496.
684 Zambardi, T., Poitrasson, F., Corgne, A., Meheut, M., Quitte, G., Anand, M., 2013. Silicon isotope
685 variations in the inner solar system: Implications for planetary formation, differentiation and
686 composition. Geochimica Et Cosmochimica Acta 121, 67-83.
687 Zhang, J.J., Dauphas, N., Davis, A.M., Leya, I., Fedkin, A., 2012. The proto-Earth as a significant
688 source of lunar material. Nature Geoscience 5, 251-255.
689